Multivariate analysis of resting state fMRI in major depression using SeedPLS

R. C. Craddock[1], S. Y. Masalovich[2], S. J. Peltier[3], X. Hu[3], H. S. Mayberg[2]

[1]School of Electrical and Computer Engineering, Georgia Institute of Technology, Atlanta, Georgia, United States, [2]School of Medicine, Emory University, Atlanta, Georgia, United States, [3]School of Biomedical Engineering, Georgia Institute of Technology/Emory University, Atlanta, Georgia, United States

INTRODUCTION

Resting state imaging studies of major depression conducted with positron emission tomography (PET) have indicated abnormalities in metabolism in the prefrontal and subgenual cortex [1,2,3,4]. Further resting state PET studies have demonstrated consistent involvement of subgenual cortex (Cg25) in acute sadness and antidepressant treatment effects, suggesting a critical role for this region in modulating negative mood states [4,5,6]. This study extends these results to resting state functional magnetic resonance imaging (fMRI) using the SeedPLS technique developed by McIntosh [7]. Due to the implication of Cg25 as a central modulator of depression, it has been chosen as the seed region of interest.

METHODS

3 subjects with depression as diagnosed by Structural Clinical Interview for the DSM-IV and 3 healthy controls underwent seven minute fMRI scans while quietly resting. These experiments were conducted on a 3T Siemens Trio scanner. A Z-SAGA [8] pulse sequence (single-shot zshim to recover areas affected by susceptibility artifact) was used to acquire 210 axial image volumes (20, 4mm thick slices) in each run with an in-plane resolution of 3.44mm x 3.44mm. Pulse sequence parameters were TR/TE/FA/FOV of 2000 ms/35 ms/90°/22 cm. The first 7 and last 3 images were discarded due to MR signal instability. Further data preprocessing was performed in SPM2 (www.fil.ion.ucl.ac.uk/spm/software/spm2). The images were first motion corrected; none of the subjects had a displacement greater then 3mm in a single direction (x,y,z). Next the images were slice-timing corrected, then transformed into MNI space and smoothed using a 6mm FWHM isotropic Gaussian kernel.

SeedPLS [7] was implemented using MATLAB (www.mathworks.com). The time series for each voxel of each subject were linearly de-trended and low-pass filtered < 0.1 Hz using a 8th order Butterworth filter, in order to avoid high frequency sources of noise and keep those frequencies shown to contribute to low-frequency functional connectivity [9]. Then the time series were correlated with the time series from Cg25 (8mm, 16mm,-8mm) to create a functional connectivity map for each subject. These maps were then compared using two different analyses. In the first analysis, the connectivity maps were first averaged within group. The global mean image was then subtracted from the averaged connectivity maps. The result was then decomposed using singular value decomposition. The resulting singular images were scaled by multiplying them by their respective singular value. The vector product was computed between each functional image and each singular image and is interpreted as each singular image's contribution to each connectivity map. The second analysis is similar to the first except that the connectivity maps were not averaged within groups.

For the first analysis the statistical significance of each singular image was determined by 9 permutations of a permutation test (with 3 subjects in each group only 9 permutations are possible). 36 bootstraps (maximum number possible) were used to estimate the standard error for each voxel. Since there is no grouping applied in the second analysis, the permutation test cannot be employed. For this analysis only 150 (maximum number possible) bootstraps were employed. Activation was defined as voxel clusters with intensity twice the estimated standard error with a contiguity threshold of at least 4 connecting voxels. If the underlying data are Gaussian the intensity threshold would correspond to a z-score of 2 and $p < 0.05$.

RESULTS AND DISCUSSION

The results of the first analysis completed show a significant ($p<0.10$) difference between functional connectivity maps of controls (1, 2, 3) compared to depressed (4, 5, 6) (Fig. 1). The singular images indicate that the amygdala, anterior insula, thalamus, orbital and medial frontal cortex, and the rostral and dorsal anterior cingulate are functionally connected to the subgenual cingulate with an inverse relationship between patients and controls (top row of Fig. 2). The scores from the second analysis indicate heterogeneity in the depressed subjects (Fig. 3). The first three singular images explain 85.73% of the total variance and each discriminate between a single depressed subject and the rest of the subjects. Singular images 1 and 3 (2nd and 4th row of Fig. 2) indicate a similar pattern between subjects 4 and 5 (depressed) with a negative relationship between Cg25 and the frontal, insular, and cingulate regions. Singular image 2 shows a distinct pattern with a predominant Cg25-rostral cingulate pattern with little to no relationship between Cg25 and frontal or insular regions (third row of Fig 2).

This pilot study illustrates that low-frequency functional connectivity in BOLD fMRI is able to discern patterns that differentiate between depressed subjects and controls. We plan to incorporate more subjects in the near future in order to increase the significance of these findings.

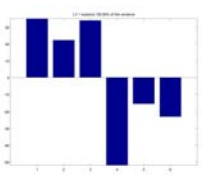

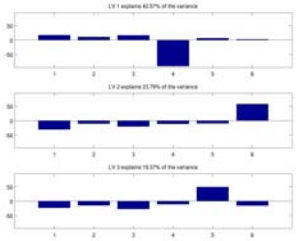

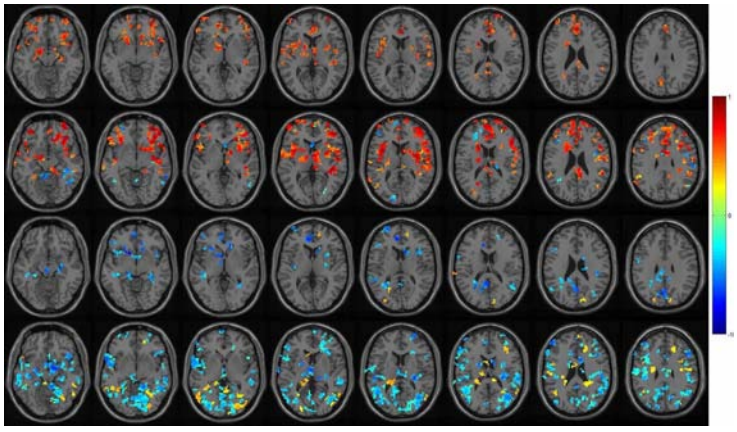

Figure 1 (above left) illustrates the subject scores for the singular image of the first analysis presented.
Figure 2 (above right) illustrates the subject scores for the singular images of the second analysis presented. Subjects 1-3 are controls and 4-6 are depressed in both figures.
Figure 3 (right) depicts 4mm slices (l-r) from -9mm to +33mm. Top is the singular image from the first analysis. The bottom three are in order from the second analysis.

REFERENCES: [1] Videbech P. 2000. Acta. Psychaitr. Scand., 101:11. [2] Mayberg HS. 2003. Neuroimaging Clin N Am., 13:805. [3] Mayberg HS. 1997. J. Neuropsychiatry Clin. Neursci., 9:471. [4] Mayberg HS. 1999. Am. J. Psychiatry, 156: 675. [5] Seminowicz DA. 2004. NeuroImage., 22: 409. [6] Mayberg HS. 2005. Neuron. 45:651. [7] McIntosh AR. 2004. NeuroImage, 23: S250. [8] Heberlein KA. 2004. Magn. Reson Med., 51: 212. [9] Cordes D. 2001. AJNR Am J Neuroradiol, 22:1326.

Acknowledgements: This work was supported in part by NIH Grant R01 EB002009 and NIMH Grant P50 MH058922.